Bioengineering

AIMS Bioengineering, 12(3): 357–369.
DOI: 10.3934/bioeng.2025016
Received: 06 February 2025
Revised: 10 June 2025
Accepted: 03 July 2025
Published: 17 July 2025

https://www.aimspress.com/journal/Bioengineering

Research article

Development of a novel *In Vitro* Co-culture system for discrete subaortic stenosis

Pengfei Ji[1,2,3,4], Sunita Brimmer[1,2,3,4], Jeffrey S. Heinle[2,3,4,5], Jane Grande-Allen[6], Ravi K. Birla[1,2,3,4,5,#] and Sundeep G. Keswani[1,2,3,4,5,*]

[1] Laboratory for Regenerative Tissue Repair, Texas Children's Hospital, Houston, Texas, USA
[2] Center for Congenital Cardiac Research, Texas Children's Hospital, Houston, Texas, USA
[3] Division of Congenital Heart Surgery, Texas Children's Hospital, Houston, Texas, USA
[4] Department of Surgery, Baylor College of Medicine, Houston, Texas, USA
[5] Division of Pediatric Surgery, Department of Surgery, Texas Children's Hospital, Houston, Texas, USA
[6] Department of Bioengineering, Rice University, Houston, Texas, USA

Correspondence: Email: keswani@bcm.edu.

Joint Senior Authors.

Abstract: Discrete subaortic stenosis (DSS) is a severe congenital heart condition that results in the formation of a fibrous membrane in the left ventricular outflow track (LVOT). While DSS is surgically treated, it is frequently associated with a high rate of recurrence, necessitating multiple surgeries. The surgical burden of DSS can be reduced by implementing targeted drug therapies based on the underlying molecular mechanisms. There are multiple cell types within the LVOT, consisting of fibroblasts and endocardial endothelial cells (EECs), organized in a complex 3D space. Our objective of this study was to develop a 3D system for the concurrent coculture of fibroblasts and EECs, as a first step in the development of a tool to better understand the cellular communication between these two cell types. To accomplish this objective, we used extrusion-based bioprinting to fabricate 3D discs. Extrusion-based bioprinting was used to generate a 3D disc with fibroblasts and EECs distributed in different configurations within the 3D disc. We demonstrated that the fibroblasts and the EECs maintained viability as a function of time for up to 4 days under static (this is extra spacing here)

conditions. Furthermore, to simulate the wall shear stress conditions in the LOVT, a cone and plate bioreactor was used in conjunction with the 3D bioprinted disc for a culture period of up to 24 hours. We demonstrated that EECs maintained CD31 expression for up to 24 hours when cultured within the 3D discs under conditions of elevated shear stress. Collectively, our results demonstrate the initial success of the 3D bioprinted disc model as a potential tool for studying DSS. While additional optimization and validation studies are required, the model described in this study has the potential to provide insight into the underlying molecular mechanism of DSS disease phenotype and lead to the development of targeted therapies for the treatment of this challenging congenital heart condition.

Keywords: Discrete subaortic stenosis; bioreactor; bioprinting; coculture; shear stress

1. Introduction

Children with discrete subaortic stenosis (DSS) experience a narrowing of the left ventricular outflow tract (LVOT), caused by the formation of a fibromembranous tissue. This blockage increases the pressure in the LVOT, which is just below the aortic valve [1]. DSS is an uncommon occurrence in children with congenital heart defects, with a prevalence rate of around 6%. The pathogenesis of DSS is hypothesized to begin during the first 10 years of life [1]. Symptoms include chest pain, heart failure, and syncope, with about 50% of patients having a heart murmur that grows with age [1]. The morphology of the lesions associated with DSS typically consists of a fibromuscular tissue ring or a localized protrusion of fibrous tissue [1]. It is believed that the condition is initiated by geometric abnormalities in the LVOT, which generate turbulent blood flow and altered shear forces that trigger a fibrotic response [2]. Although surgical resection of the membranes provides relief, there is a high risk of recurrence (20–30%) in what is defined as an aggressive DSS phenotype, with female sex being a risk factor [1]. Without intervention, DSS can lead to left ventricular hypertrophy, aortic regurgitation, endocarditis, arrhythmias, and in extreme cases, death [3].

Surgical correction of the membrane has been demonstrated to be a viable option for eliminating obstruction. The membrane will either be removed via myomectomy, or just the fibrous tissue ring resected [1]. However, it has the potential to pose numerous risks, such as those associated with anesthesia, sternotomy, and heart bypass. In certain cases of aggressive DSS, open-heart surgery poses a high risk to patients, and in these cases, percutaneous balloon dilation is preferred [1]. This procedure provides relief for a few years, and then the surgery must be performed again, defined as an aggressive phenotype [1]. These surgical approaches only provide temporary relief, and most patients will require reoperation due to regrowth of the fibrous membrane and also require long-term follow-up care [1].

Although 2D cell culture studies enable researchers to understand the biology and morphology of cells and tissues, such studies are limited in the ability to promote cellular communication between different cell types and with the extracellular matrix. Three-dimensional models overcome these limitations and enable cellular communication and more accurately mimick disease conditions like DSS [4,5]. With 3D models, we can reproduce the functional characteristics of the heart's tissue organization and microenvironment [6–8]. As stated earlier, DSS is hypothesized to be caused by interactions between two cell types, EECs and fibroblasts [1]. Monolayer 2D cell culture systems and

models are centered around a single cell type, which is vastly different from the natural environment of the LVOT. Thus, this limitation makes it difficult to understand the mechanistic and biological properties of DSS. Therefore, we developed a 3D co-culture system to overcome the limitations of 2D monolayer cell culture systems and support functional interactions between multiple cell types and with the extracellular matrix. In addition to the 3D culture environment, the environment is critical in cell and tissue phenotypes [10].

Bioreactors are specialized apparatus designed to simulate physiological *in vivo* conditions during controlled *in vitro* culture [10]. Examples include bioreactors for electrical stimulation [11], uniaxial stretch [12], and pulsatile fluid flow [13]. In the case of DSS, wall shear stress is the most important physiological variable, and cone and plate bioreactors (CPBs) are used to simulate WSS on endothelial cells. In this study, we our objective is to develop a 3D co-culture system, for EECs and cardiac fibroblasts and also test the compatibility of the co-culture system with CPBs, thereby simulating DSS.

2. Materials and methods

Gelatin from bovine skin powder (9000-70-8), calcium chloride pellets (10043-52-4), and sodium alginate (9005-38-3) were obtained from Sigma Aldrich. A Commercial Cellink BIOX Printer (Model: S-10001-001; S/N: 202041) was used. ECM media (Sciencell, 1001) and fibroblast growth media 3 were obtained and used for cell culture (PromoCell Inc. C-23025). Moreover, we used 0.05% Trypsin EDTA (Gibco™ 25300054) to dislodge the cells from the culture plates [14].

2.1. Research design

Four types of disks were fabricated (Figure 1). The 1st group contained only EECs in all 3 layers, with 3×10^5 EECs per layer. The 2nd group contained only porcine fibroblasts in all 3 layers, 3×10^5 porcine fibroblasts per layer. The 3rd group of disks comprised 2 layers of porcine fibroblasts and 1 layer of EECs as the top layer, with the same ratio of cells per layer as the first 2 groups. Last, the 4th group of disks contained 3 layers of porcine fibroblasts and EECs dispersed throughout all 3 layers, with 1.5×10^5 EECs and 1.5×10^5 porcine fibroblasts in each layer for a total of 3×10^5 cells per layer. Cells were cultured in the disk for 48 hours and then each group was subjected to shear stress in the cone-and-plate bioreactor at 6 dynes/cm^2 for 24 hours. The cell viability was confirmed using the MTT assay, according to manufacturer's instructions. CD31 expression was quantified in group 1 discs after 1, 2, and 4 days in culture using a published protocol [15].

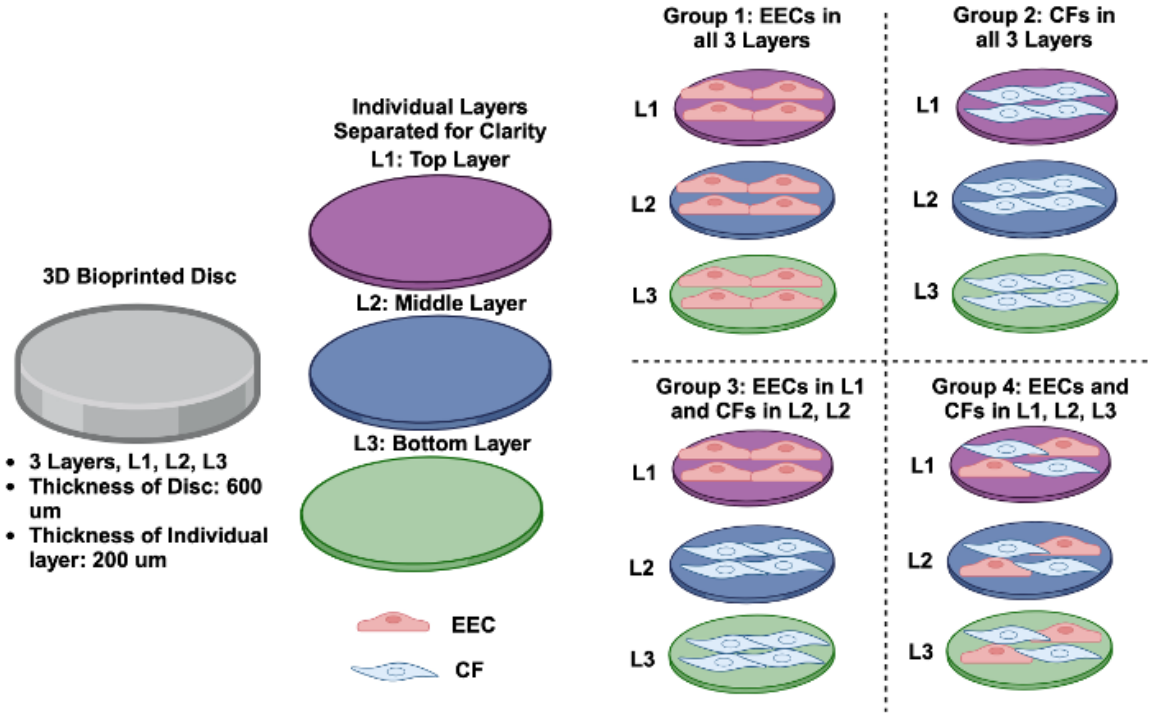

Figure 1. Experimental Design: We bioprinted a 3-layer disc, each layer 200 µm thick, resulting in a total thickness of the disc of 600 µm. For clarity, the 3 layers are shown separately and identified as L1 (top layer), L2 (middle layer), and L3 (bottom layer). The 3D disc was populated with EECs and/or CFs and divided into 4 groups. The distribution of EECs and CFs within each of the 3 layers in the 4 groups is shown in the Figure. Created with BioRender.com.

2.2. Cell culture

Porcine CFs and EECs were cultured on individual monolayers of 0.1% gelatin, seeding 5×10^5 cells. EECs and CFs were maintained in ECM media and fibroblast growth media 3, respectively. Once cells reached confluency and before trypsinization, each cell type was labeled using CellTrackers. To be more specific, the porcine EECs were labeled by GFP (ThermoFisher, Cat #Q25041MP), and porcine CFs were laveled by Texas Red (ThermoFisher, Cat # Q25021MP). The cells were detached using 0.05% Trypsin EDTA and cultured with the Celltracker-labeled cells as mentioned.

2.3. Optimization of bioink with cells

In previous studies [15], we established that 8% alginate produced the best results of reproducibility, ease of crosslinking, and appropriate stiffness. We established the appropriate seeding density of cells in alginate hydrogel using a 3-way luer lock to combine one syringe containing 1 mL of 8% alginate with a separate syringe containing 200 µL of 1×10^6 cell suspension. After printing, confocal images were acquired and used to visualize the distribution of cells within the 3D disc.

2.4. Disk fabrication

As shown in Figure 2, the disks were developed through a 4-step process. First, we created an STL file using a bioprinter that formulates a set of instructions on how to build a disk with 3D geometry through programmed printhead movements in the x, y, and z planes. The disks were 55 mm in diameter. The file was then transferred to the 3D printer, where it was sliced into layers and printed as a grid pattern. A total of 3 g of gelatin were combined with 30 mL of 0.2% $CaCl_2$, a sodium alginate crosslinking agent. After 10 minutes, the gelatin mixture was centrifuged and plated to fill the volume of the Nunclon ™ dish. Next, the cartridge containing 1 mL of alginate with 200 µL of cell suspension was attached to a stainless steel dispense tip (Nordson EFD, Cat #7018345), which was calibrated to a position 10 mm deep into the gelatin support bath. Once printing was complete, the dish was placed in the incubator for 2 hours to enable the gelatin to completely melt. Thereafter, the gelatin was aspirated, and 20 mL of media with 1% $CaCl_2$ was added to supply nutrients to the cells embedded in the disk, enabling the disk to achieve maximum stiffness over 24 hours. The disk was then stored in the incubator.

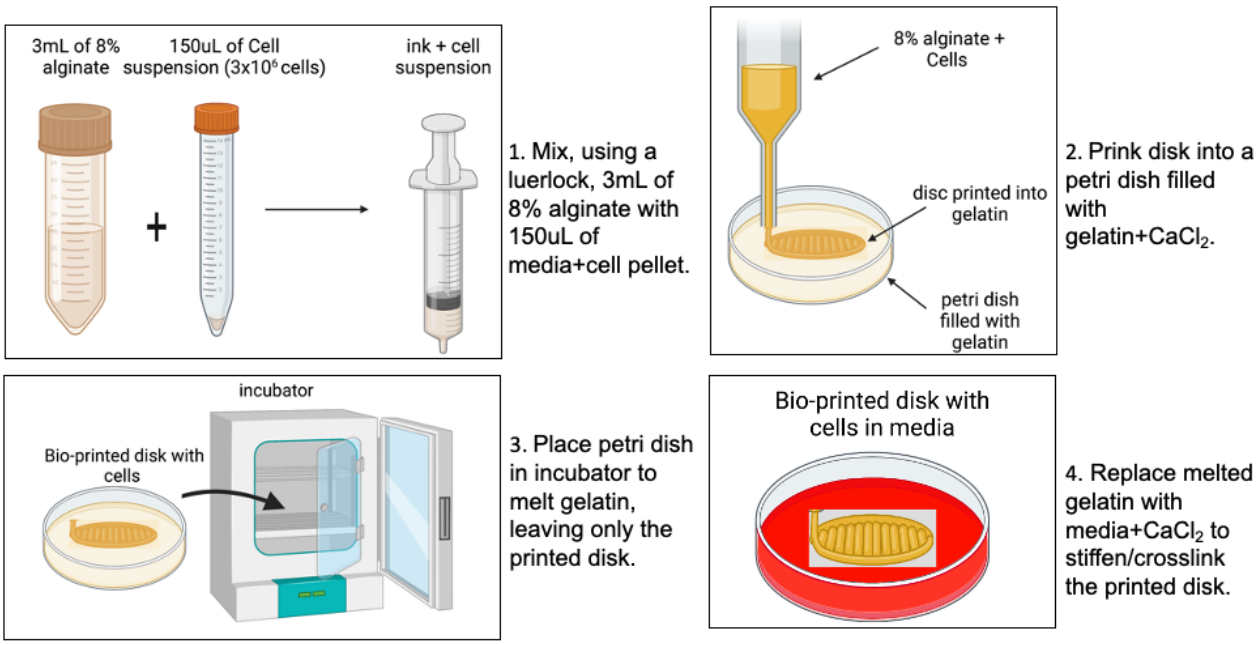

Figure 2. Methodology to Bioprint 3D Discs: A solution of 8% alginate is mixed with a cell suspension, consisting of either EECs, CFs, or both. The cell suspension is loaded onto an extrusion-based bioprinter and used to bioprint a 3D disc within a gelatin support bath. The printed structure is incubated at 37 °C to enable the gelatin support bath to dissolve. The bioprinted disc with the cells is then cultured in a cell culture incubator. Created with BioRender.com.

2.5. Application of shear forces

We used the cone and plate bioreactors to apply the fluid shear stress experienced by EECs in the LVOT of patients with DSS. The CPB system operates based on the following principle: An inverted cone is positioned above a stationary flat plate, creating a narrow gap through which fluid flows [16,17]. This arrangement ensures the distribution of uniform shear stress across the surface [18]. To control the fluid flow, a magnetic stir plate was used, which enabled the adjustment of the cone's angular velocity by modifying the revolutions per minute (RPM) setting on the control unit. This mechanism enables precise manipulation of the shear stress experienced by the EECs in the CPB system [18–20]. The magnitude of the shear stress was fixed at 6 dyne/cm^2, which represents physiological flow conditions. To accomplish a shear stress of 6 dyne/cm^2, we adjusted the rotational speed of the cone and plate bioreactor to 105 RPM.

2.6. Fixing the disks and confocal microscopy

The disks containing cells were initially cut in half or small pieces and transferred onto a 6-well plate, and then fixed using a 4% paraformaldehyde solution for 24 hours. Following the fixation, the paraformaldehyde solution was removed, and the disks were washed three times with PBS. The disks were subsequently imaged and processed using a CellVoyager CV8000 Yokogawa confocal scanner microscope. For imaging, a z-depth range of -150 to 550 μm was selected, with a scanner layer thickness of 6.5 μm. The lasers used were 640 nm for PCF labeled with Texas Red and 488 nm for EEC labeled with GFP. The objective lens chosen for visualizing the discs was the 4× lens. The acquired images were then merged and analyzed using CellPathfinder (a high-content analysis software developed by Yokogawa) to generate 2D or 3D aligned images.

3. Results

Bioprinting 3D Disc: Our first task was to demonstrate that we could successfully bioprint a 3D disc and have control over the different layers within the disc. As shown in Figure 3, a blue dye was added to the bioink used to bioprint the top layer to differentiate this layer from the underlying two layers.

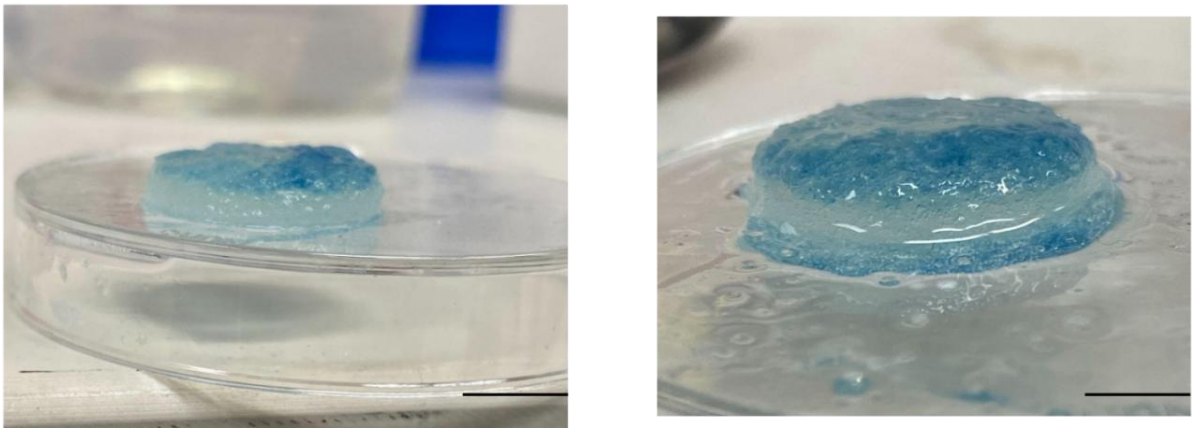

Figure 3. Feasibility of Disc Formation: The bioink was colored with a blue dye to print the top layer of the disc only to differentiate the top layer from the lower two layers. The scale bar represents 500 microns.

Confirming Viability of Cells within 3D Discs: Our next task was to confirm the cell viability during 3D culture within the bioprinted disc under static conditions. We used the MTT assay and demonstrated no loss of cell viability after 2 and 4 days in culture (Figure 4). Furthermore, we noted a trend toward an increase in cell number after 4 days in culture, though these results were not statistically significant.

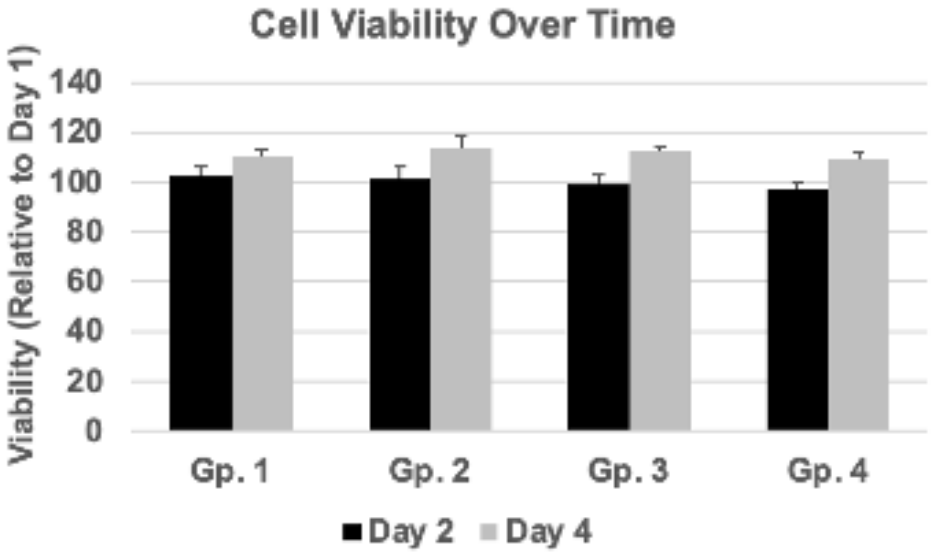

Figure 4. Viability of Cells in 3D Discs: The MTT assay is used to measure cell viability and proliferation after 2 and 4 days relative to day 1. No statistical differences are noted between groups. N = 3 per group.

Confirming Cell Labeling in 2D Monolayer Cultures: Prior to using EECs and CFs for 3D bioprinting, we developed a 2-color labeling system to differentiate and trace these two cells within the 3D bioprinted disc. To accomplish this objective, porcine EECs were labeled with GFP, and CFs were labeled with Texas Red. The results of the labeling are presented in Figure 5 and demonstrate efficacy in our labeling system, with the EECs colored green and the CFs colored red.

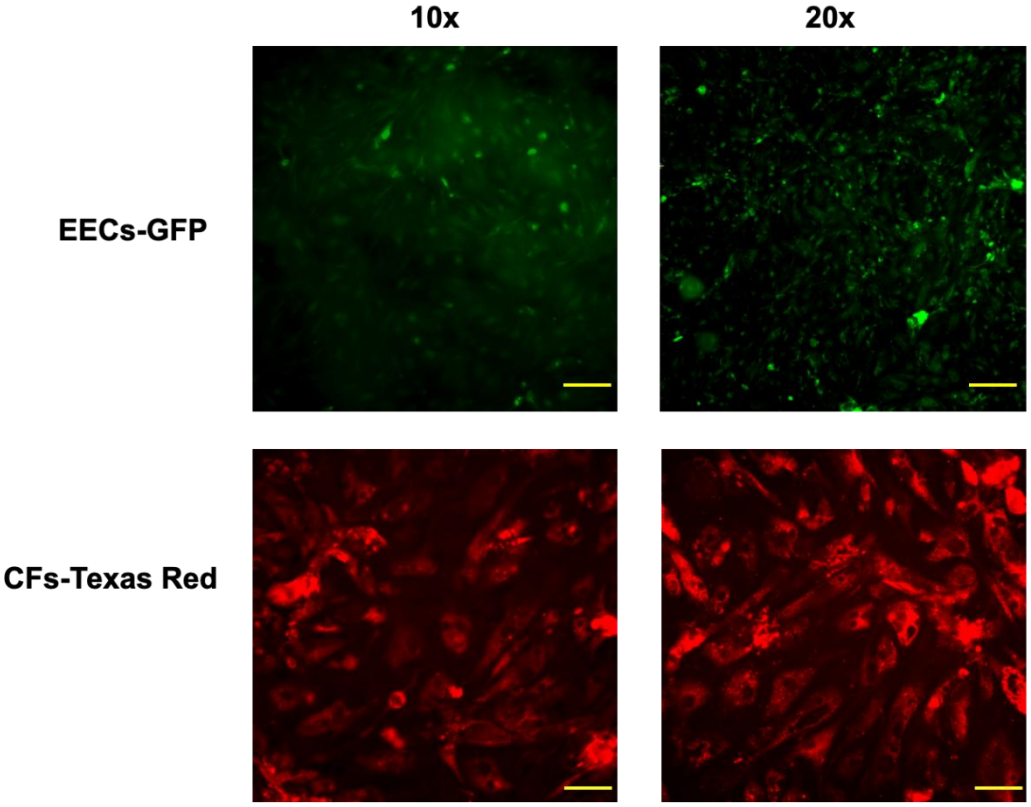

Figure 5. Two-Color Labeling System During 2D Monolayer Culture: EECs are labeled with GFP, and CFs are labeled with Texas Red to differentiate the two cell types. Representative images of EECs and CFs are shown during 2D monolayer cultures. The scale bar represents 500 microns at 10× and 250 microns at 20×.

Bioprinted 3D Discs with EECs and CFs: The cells were transferred from the monolayers to the 3D disks using the ECM medium for the porcine EEC, and porcine fibroblasts were maintained in fibroblast growth media 3. After culturing for 72 hours, the bioprinted discs were fixed, and the images were taken by Yokogawa CellVoyager CV8000 under the 4x objective, as shown in Figure 6. The images were from different z-depths, such as −50, 100, 350, and 500 μm, and the cells were widely distributed in the monolayers. Representative images from z-depths of 100 and 200 μm are shown, with GFP labeled EECs and Texas-Red labeled CFs distributed throughout the discs.

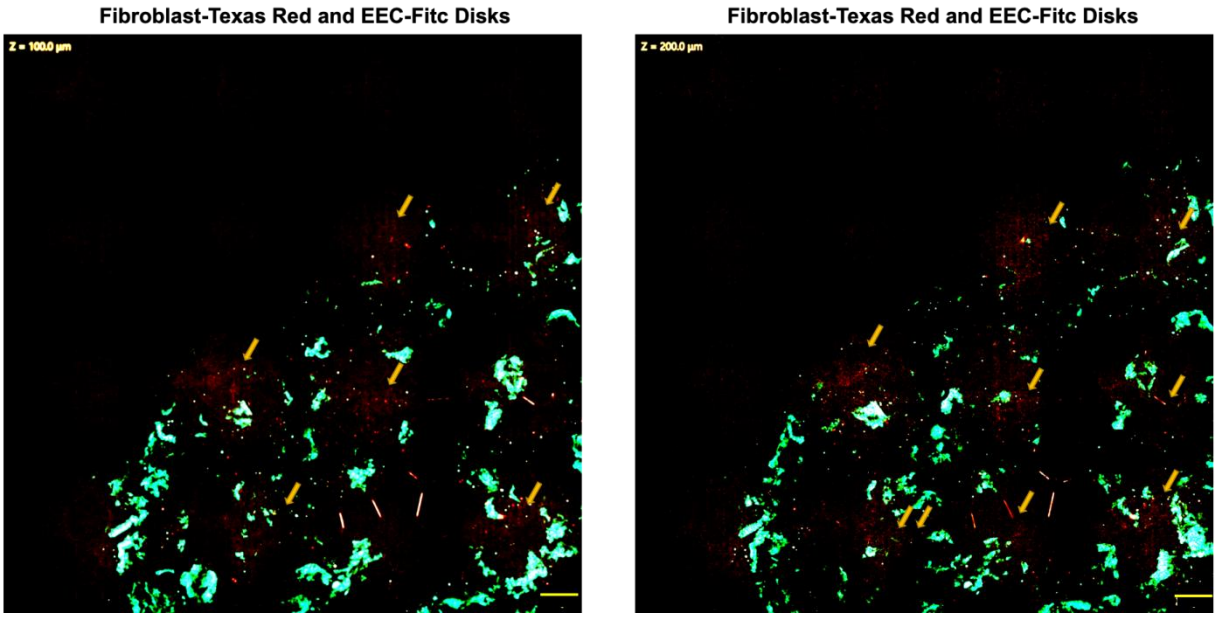

Figure 6. Two-Color Labeling System During 3D Culture in Disc: 3D bioprinted discs are fabricated using GFP labeled EECs and Texas Red labeled CFs. After 24 hours of bioreactor culture, the 3D discs are imaged, and EECs and CFs are seen throughout the discs at z-depths of 100 µm and 200 µm. The scale bar represents 500 microns.

Confirmation of CD31 Expression in Group 1: We confirmed the phenotype of EECs in group 1, as they contained only EECs. CD31 expression was used as an indicator of the cell phenotype to confirm that the 3D culture environment supports the culture of these cells. As noted in Figure 7, there was no significant difference in CD31 expression over the 4-day culture period, validating the use of the 3D bioprinted disc model.

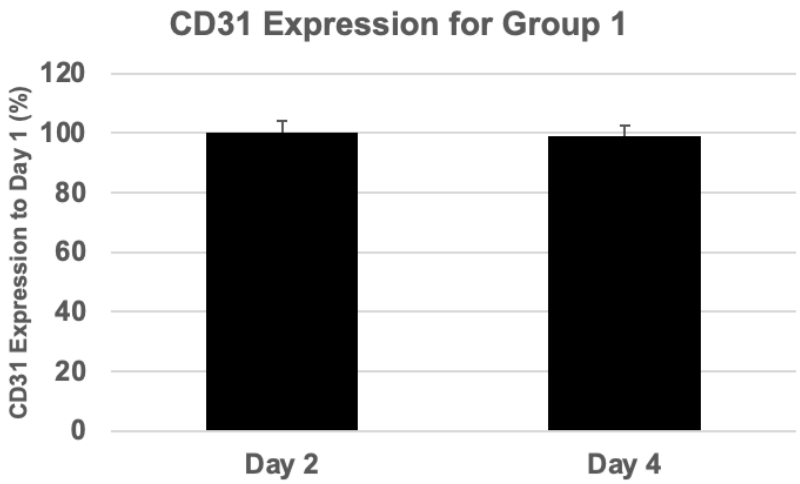

Figure 7. Cell Phenotype for Group 1: CD31 expression of EEC within the 3D bioprinted discs is quantified after 2 and 4 days in culture and normalized relative to day 1 expression.

4. Discussion

DSS is a very serious congenital heart condition and one that adversely affects thousands of patients across the globe. There is no known cure for this condition, and the underlying molecular mechanism remains unknown. However, it is speculated that changes in the WSS and subsequent response of EECs and CFs play a central role in mediating the DSS phenotype. Thus, understanding the crosstalk between EECs and CFs is essential to develop a better understanding of the DSS phenotype and subsequently develop therapies to treat this condition. We were attentive to this need, and the study was designed to develop a 3D co-culture system for EECs and CFs in the presence of a cone and plate bioreactor.

We made use of a commercial extrusion based bioprinter, the BioX, to generate 3D discs. The dimensions were selected as 55 mm diameter to support compatibility of the discs with the cone and plate bioreactor. The thickness of the disc was 600 microns and consisted of 3 layers, each of 200-micron thickness. Each of the 3 layers could be potentially populated with a different cell type, if needed.

Our preliminary experiments showed that labeled porcine EECs and CFs remained viable after being labeling with a cell tracker and transferred to a single-layer disk. Observation of living cells with a Leica microscope confirmed the successful labeling and survival of different cell types. In addition, images of Yokogawa CellVoyager CV8000 at different z depths showed that the cells were widely distributed within a single-layer disk, indicating their ability to adhere and proliferate on the disk surface. The survival of mixed CFs and EECs in multilayer disks was investigated with encouraging results. Yokogawa CellVoyager CV8000 images showed that CFs - Texas Red and EEC-GFP cells co-existed and were viable inside the disks after 48 hours. Importantly, the different cell numbers observed at different Z-depths indicate a pattern of differential potential distribution within the multilayer disc.

The simulation of WSS using cone and plate bioreactors has provided valuable insights into the mixed cell populations under conditioning medium. There were significant differences in cell distribution between the control group and the experimental group after 24 hours of bioreactor treatment. Moreover, Yokogawa CellVoyager CV8000 images showed that disks exposed to bioreactor processing showed a wider distribution of cells compared to controls. This observation suggests that the dynamic fluid environment promotes the dispersion of cells within the disk. In addition, a reduction in the number of cells in the petri dish after bioreactor treatment, particularly CFs labeled with Texas red, may indicate potential cell detachment or altered cell survival ratio under the shear stress conditions.

The use of bioreactors in co-culture systems can significantly affect cell distribution, as indicated by the results. The decrease in the number of cells observed in the bioreactor-treated samples suggests that shear stress caused by the flow dynamics of the bioreactor may lead to cell detachment. This finding is consistent with other research and highlights the importance of optimizing bioreactor conditions to maintain cell adhesion and prevent cell loss during culture. Thus, understanding the effects of shear stress on cell behavior is critical to successfully implementing a co-culture system in DSS.

This model system has applications in the study of DSS and will increase our understanding of the underlying molecular mechanism of DSS. In DSS, elevated WSS act on EECs, and these cells can respond to disturbed flow environments by a number of mechanisms, including endo-MT, secretion of

proinflammatory and profibrotic cytokines, and an increase in cell proliferation. However, the mechanism remains unknown. The system that we develop here can be used as an important tool to study the changes in EEC phenotypes in response to elevated shear stress. The second step in the cascade is the response of the CFs. These cells respond by an increase in fibrosis, promoting ECM production that results in the formation of a fibrotic membrane in DSS patients. The mechanism by which the fibrotic cascade is initiated in CFs remains unknown. One hypothesis is that profibrotic cytokines secreted by EECs in response to elevated WSS act on the CFs, promoting fibrosis. However, this hypothesis has not been tested as no tools are available to accomplish this. However, our model enables us to accomplish this objective.

There are limitations to our model. The first limitation is the use of only 2 cell types to recapitulate the anatomy of the LVOT. The LVOT is multicellular and consists of numerous cell types acting in tandem to maintain functions and phenotypes. Examples include the presence of immune cells and other interstitial cells besides CFs. A more comprehensive model is required to simulate LVOT function. Our model simulates the partial anatomy of the LVOT, which includes the ECCs and the CFs. Although our model is powerful, these limitations should be acknowledged. A second limitation of our model is the lack of a vasculature or perfusion apparatus for continuous media flow. All tissue, including the LVOT, is supported by a robust network of blood vessels that serve to provide continuous blood flow. The vasculature also provides important information about changes in cell/tissue damage and recovery; this is an important aspect of LVOT hemostasis that is lacking in our model. While our model is 3D in nature, it lacks a vasculature, and this limitation should be acknowledged.

By providing a more comprehensive and versatile approach, co-culture systems have the potential to create organizational structures that better mimic the complexity and function of native tissues. This approach enables researchers to study cell-cell interactions, signaling pathways, and tissue development in a more physiologically relevant way. Ultimately, it provides more efficient and functional tissue structures to improve the treatment for DSS patients.

5. Conclusion

Our results demonstrate the successful survival, distribution, and interaction of mixed cell populations on a 3D bioreactor disk, as well as their behavior under bioreactor treatment. The results show the viability of the labeled cells and their ability to proliferate in single - and multilayer (disks) cultures. The use of bioreactors affects cell distribution and results in a decrease in cell numbers, which may be due to detachment caused by shear stress. These findings contribute to the understanding of cell behavior in engineered systems and have implications for DSS applications.

Acknowledgement

This work with supported by an NIH R01 Grant number 5R01HL140305. This work was supported by funding from the Lew and Laura Moorman Family Foundation to SGK. The authors would like to thank financial support from the Division of Congenital Heart Surgery, Texas Children's Hospital, Houston, TX.

Conflict of interest

The authors declare no conflict of interest related to this study.

References

1. Masse DD, Shar JA, Brown KN, et al. (2018) Discrete subaortic stenosis: perspective roadmap to a complex disease. *Front Cardiovasc Med* 5: 122. https://doi.org/10.3389/fcvm.2018.00122
2. Shar JA, Brown KN, Keswani SG, et al. (2020) Impact of aortoseptal angle abnormalities and discrete subaortic stenosis on left-ventricular outflow tract hemodynamics: preliminary computational assessment. *Front Bioeng Biotechnol* 8: 114. https://doi.org/10.3389/fbioe.2020.00114
3. Mohan JC, Shukla M, Mohan V, et al. (2016) Acquired discrete subaortic stenosis late after mitral valve replacement. *Indian Heart J* 68 (Suppl 2): S105–S109. https://doi.org/10.1016/j.ihj.2016.01.001
4. Birla RK, Williams SK (2020) 3D bioprinting and its potential impact on cardiac failure treatment: An industry perspective. *APL Bioeng* 4: 010903. https://doi.org/10.1063/1.5128371
5. Birla RK (2020) A methodological nine-step process to bioengineer heart muscle tissue. *Tissue Cell* 67: 101425. https://doi.org/10.1016/j.tice.2020.101425
6. Abbasgholizadeh R, Islas JF, Navran S, et al. (2020) A highly conductive 3D cardiac patch fabricated using cardiac myocytes reprogrammed from human adipogenic mesenchymal stem cells. *Cardiovasc Eng Technol* 11: 205–218. https://doi.org/10.1007/s13239-019-00451-0
7. Patel NM, Birla RK (2018) The bioengineered cardiac left ventricle. *ASAIO J* 64: 56–62. https://doi.org/10.1097/MAT.0000000000000642
8. Hogan M, Souza G, Birla R (2016) Assembly of a functional 3D primary cardiac construct using magnetic levitation. *AIMS Bioeng* 3: 277–288. https://doi.org/10.3934/bioeng.2016.3.277
9. Williams SK, Birla RK (2020) Tissue engineering solutions to replace contractile function during pediatric heart surgery. *Tissue Cell* 67: 101452. https://doi.org/10.1016/j.tice.2020.101452
10. Khait L, Hecker L, Blan NR, et al. (2008) Getting to the heart of tissue engineering. *J Cardiovasc Transl Res* 1: 71–84. https://doi.org/10.1007/s12265-007-9005-x
11. Mohamed MA, Islas JF, Schwartz RJ, et al. (2017) Electrical stimulation of artificial heart muscle: a look into the electrophysiologic and genetic implications. *ASAIO J* 63: 333–341. https://doi.org/10.1097/MAT.0000000000000486
12. Birla RK, Huang YC, Dennis RG (2007) Development of a novel bioreactor for the mechanical loading of tissue-engineered heart muscle. *Tissue Eng* 13: 2239–2248. https://doi.org/10.1089/ten.2006.0359
13. Khait L, Hecker L, Radnoti D, et al. (2008) Micro-perfusion for cardiac tissue engineering: development of a bench-top system for the culture of primary cardiac cells. *Ann Biomed Eng* 36: 713–725. https://doi.org/10.1007/s10439-008-9459-2
14. Brown KN, Phan HKT, Jui EL, et al. (2023) Isolation and characterization of porcine endocardial endothelial cells. *Tissue Eng Part C Methods* 29: 371–380. https://doi.org/10.1089/ten.TEC.2023.0009

15. Brimmer S, Ji P, Birla RK, et al. (2024) Development of novel 3D spheroids for discrete subaortic stenosis. *Cardiovasc Eng Technol* 15: 704–715. https://doi.org/10.1007/s13239-024-00746-x
16. Chavarria D, Georges KA, O'Grady BJ, et al. (2025) Modular cone-and-plate device for mechanofluidic assays in Transwell inserts. *Front Bioeng Biotechnol* 13: 1494553. https://doi.org/10.3389/fbioe.2025.1494553
17. Ye C, Ali S, Sun Q, et al. (2019) Novel cone-and-plate flow chamber with controlled distribution of wall fluid shear stress. *Comput Biol Med* 106: 140–148. https://doi.org/10.1016/j.compbiomed.2019.01.014
18. Sucosky P, Padala M, Elhammali A, et al. (2008) Design of an ex vivo culture system to investigate the effects of shear stress on cardiovascular tissue. *J Biomech Eng* 130: 035001. https://doi.org/10.1115/1.2907753
19. Shar JA, Keswani SG, Grande-Allen KJ, et al. (2022) Significance of aortoseptal angle anomalies to left ventricular hemodynamics and subaortic stenosis: a numerical study. *Comput Biol Med* 146: 105613. https://doi.org/10.1016/j.compbiomed.2022.105613
20. Shar JA, Keswani SG, Grande-Allen KJ, et al. (2021) Computational assessment of valvular dysfunction in discrete subaortic stenosis: a parametric study. *Cardiovasc Eng Technol* 12: 559–575. https://doi.org/10.1007/s13239-020-00513-8

AIMS Press